Materials Research Proceedings **17** (2020) 1-8 https://doi.org/10.21741/9781644901038-1

Failure Prediction of Spool Control Valve using CFD Simulation

DOMAGALA Mariusz[1 a *], BIKASS Saeed[2], FABIS-DOMAGALA Joanna[1], MOMENI Hassan[2] and FILO Grzegorz[1]

[1] Cracow University of Technology, Institute of Applied Informatics, Al Jana Pawla II 37,31-841 Cracow, Poland

[2] Western Norway University of Applied Sciences, Department of Mechanical and Marine Engineering, Inndalsveien 28, 5063 Bergen, Norway

[a] domagala@mech.pk.edu.pl

Keywords: Failure Prediction, Spool Control Valve, CFD Simulation

Abstract. Spool control valves play an important role in fluid power systems and required high reliability. Prediction of possible failures for such valves is a key issue. According to research most of failures which may appear are caused by contaminated fluid. Contaminants of fluid may cause erosion of metallic surfaces or cavitation wear. Both types of wear may be predicted by using CFD simulation tools and multiphase flow which includes phase changes and possibility of simulation of flow with solid particles.

Introduction

Failures prediction for hydraulic valve is very important issue due to the fact that its malfunction may cause human injuries or environmental pollution. Among all causes of hydraulic systems failures, contamination of hydraulic fluid is one of the most common. It is estimated that majority (up to 90%) of failures is caused by contamination of hydraulic fluid which might be solid particles (remaining of wear or dust) or chemical agents (liquids or gases). It is not possible to prevent hydraulic fluid against contamination even using sophisticated filtration systems. Contamination may appear in the hydraulic systems internally as a normal process of operation, as a result of wear of hydraulic components. Solid particles in very specific flow conditions, very often with high flow velocity, gain momentum from fluid and may cause erosive wear inside components. Additionally, fluid flowing inside hydraulic components, particularly inside valves, rapidly changing direction and velocity what may lead to sudden pressure drop, below saturation pressure and cavitation and wear of surface of valve components. Both type of wears: erosive and cavitation has been investigated from decades on experimental way. Recent development of simulation methods (in particular computational fluid dynamics: CFD) allows to predict wear before their occurrence [1-4]. This paper presents research on flow inside spool control valve for two cases. First one is multiphase flow with contaminants (metallic particles) while the second deals with phase change flow (cavitation). Both simulations might be used for predicting spool valve wear.

The failure prediction presented here can be used in analogous issues, both related to fluid flows (e.g. biotechnology [5, 6], heat flows [7]) and in the field of solid materials engineering (e.g. materials science [8, 9] and design of medical implants [10]) as well as enhancement of surface layers [11], where the aim is to improve tribological properties [12] and fatigue resistance [13]. It is certain that this will have an impact on related methods of management

optimization [14, 15] and data analysis [16, 17] as well as CFD numerical methods [18-20] aimed at erosion modeling [21, 22] and associated failure analysis methods [23, 24].

Modelling of erosion and cavitation

The wear caused by impact of solid particles on walls for metals is a function of impact angle and particle velocity [25]:

$$E = kV_p^n f(\gamma) \tag{1}$$

where:

E – dimensionless mass (mass of eroded wall material divided by the mass of particle),
V_p – particle velocity,
n – exponent value which for metals is between 2.3 and 2.5,
$f(\gamma)$ – function of impact angle.

One of the models that describes rate of wear is Finnie model [26] :

$$E = kV_p^2 f(\gamma) \tag{2}$$

where:

$$f(\gamma) = \frac{1}{3}cos^2(\gamma)\ if\ tan(\gamma) > \frac{1}{3} \tag{3}$$

$$f(\gamma) = sin(2\gamma) - 3sin^2(\gamma)\ if\ tan(\gamma) > \frac{1}{3} \tag{4}$$

Other model which describes erosion rate is Tabakoff and Grant [27]:

$$E = k_1 f(\gamma) V_p^2 cos^2(\gamma)\ [1 - R_T^2] + f(V_{PN}) \tag{5}$$

where:

$$f(\gamma) = \left[1 + k_2 k_{12} sin\left(\gamma \frac{\frac{\pi}{2}}{\gamma_0}\right)\right]^2 \tag{6}$$

$$R_T = 1 - k_4 V_p sin\,(\gamma) \tag{7}$$

$$f(V_{PN}) = k_3 \left(V_p sin\,(\gamma)\right)^4 \tag{8}$$

$$k_2 = \begin{cases} 1.0\ if\ \gamma \le 2\gamma_0 \\ 0\ if\ \gamma > 2\gamma_0 \end{cases} \tag{9}$$

k_1, k_{12} – constants.

Simulation of particles in continuous fluid in CFD is treated as two phases flow: discreet one (particles) and continuous one (fluid). Discreet particles are tracked into fluid domain during fluid flow. Equation of motion for a single particle according to Basset, Boussinesq and Oseen may be presented in the following way:

$$m_p \frac{dU_p}{dt} = F_D + F_B + F_R + F_{VM} + F_P + F_{BA} \tag{10}$$

where: F_D – drag force, F_B – buoyancy force, F_R – Coriolis force, F_{VM}- is inertia force of fluid occupied by particle (Virtual Mass), F_P – pressure force, F_{BA} – Basset force

The inertia force of fluid occupied by particle (Virtual Mass) is expressed by the following equation:

$$F_{VM} = \frac{C_{VM}}{2} m_F \left(\frac{dU_F}{dt} - \frac{dU_P}{dt}\right) \tag{11}$$

Transforming Eq. 10 we obtain:

$$\frac{dU_p}{dt} = \left(\frac{1}{m_p + \frac{C_{VM}}{2} m_F}\right)(F_D + F_B + F_R + F'_{VM} + F_P + F_{BA}) \tag{12}$$

where

$$F'_{VM} = \frac{C_{VM}}{2} m_F (U_F \nabla U_F) \tag{13}$$

$m_P = \frac{\pi}{6} \mathrm{d_P^3} \rho_P$ – particle mass,
$m_F = \frac{\pi}{6} \mathrm{d_P^3} \rho_F$ – fluid mass,
$\mathrm{d_p}$ – the particle diameter,
ρ_P, ρ_F – density of particle and fluid respectively.

Assuming that:

$$R_{VM} = \frac{m_P}{m_P + \frac{C_{VM}}{2} m_F} = \frac{\rho_P}{\rho_P + \frac{C_{VM}}{2} \rho_F} \tag{14}$$

Finally Eq. 10 has the following form:

$$\frac{dU_p}{dt} = \left(\frac{R_{VM}}{m_p}\right)(F_D + F_B + F_R + F'_{VM} + F_P + F_{BA}) \tag{15}$$

In generally, tendency of fluid flow to cavitation may be expressed as:

$$\mathrm{c_a} = \frac{\mathrm{p - p_v}}{0.5 \rho \mathrm{U^2}} \tag{16}$$

One of the approaches which describes bubble dynamics is The Rayleigh-Plesset formula:

$$R_b \frac{d^2 R_b}{dt^2} + \frac{3}{2}\left(\frac{dR_b}{dt}\right)^2 + \frac{2\sigma}{\rho R_b} = \frac{p_v - p}{\rho} \tag{17}$$

After neglecting surface tension and term of second order the above eq. have the following form:

$$\frac{dR_b}{dt} = \sqrt{\frac{2}{3}\left(\frac{p_v - p}{\rho}\right)} \tag{18}$$

The rate of changes of bubble volume is:

$$\frac{dV_b}{dt} = 4\pi {R_b}^2 \sqrt{\frac{2}{3}\left(\frac{p_v - p}{\rho}\right)} \tag{19}$$

The rate of changes of bubble mass is:

$$\frac{dm_g}{dt} = 4\pi {R_b}^2 \rho_g \sqrt{\frac{2}{3}\left(\frac{p_v - p}{\rho}\right)} \tag{20}$$

The number of bubbles Nb per unit volume rg is expressed by:

$$r_g = \frac{4}{3}\pi R_b^2 N_b \tag{21}$$

The total interphase mass transfer per unit volume is:

$$\dot{m}_{fg} = 3\frac{r_g \rho_g}{R_b}\sqrt{\frac{2}{3}\frac{p_v - p}{p_f}} \tag{22}$$

After including condensation to above expression have the following form:

$$\dot{m}_{fg} = 3F\frac{r_g \rho_g}{R_b}\sqrt{\frac{2}{3}\frac{p_v - p}{p_f}\mathrm{sgn}(p_v - p)} \tag{23}$$

And finally the vapor transport equation have form:

$$\frac{\partial}{\partial \mathrm{t}}(\alpha\rho_\mathrm{v}) + \nabla\cdot(\alpha\rho_\mathrm{v}\mathbf{U}_\mathrm{v}) = \mathrm{R_e} - \mathrm{R_c} \tag{24}$$

where:

R_b – bubble radius, p_v – vapor pressure, p – pressure of liquid surrounding the bubble, ρ – liquid density, ρ_g – vapor density, σ – surface tension, U_v – vapour phase velocity, α – vapor volume fraction, n – bubble number, R – phase change rate, f_v – vapor mass fraction, f_g – noncondesable gases, R_e, R_c – mass transfer source terms connected to the growth and collapse of the vapor bubbles, respectively.

Spool control valve

The spool control valve presented in Fig. 1. is used to control the direction of flow and movements speed of actuators. Position of spool is determined by proportional solenoids which allows to control both direction of flow and receivers movement speed. Return to neutral position (any receiver is supplied) is provided by two springs. The shape of the spool determines flow configuration (connections between ports: P, T, A, B).

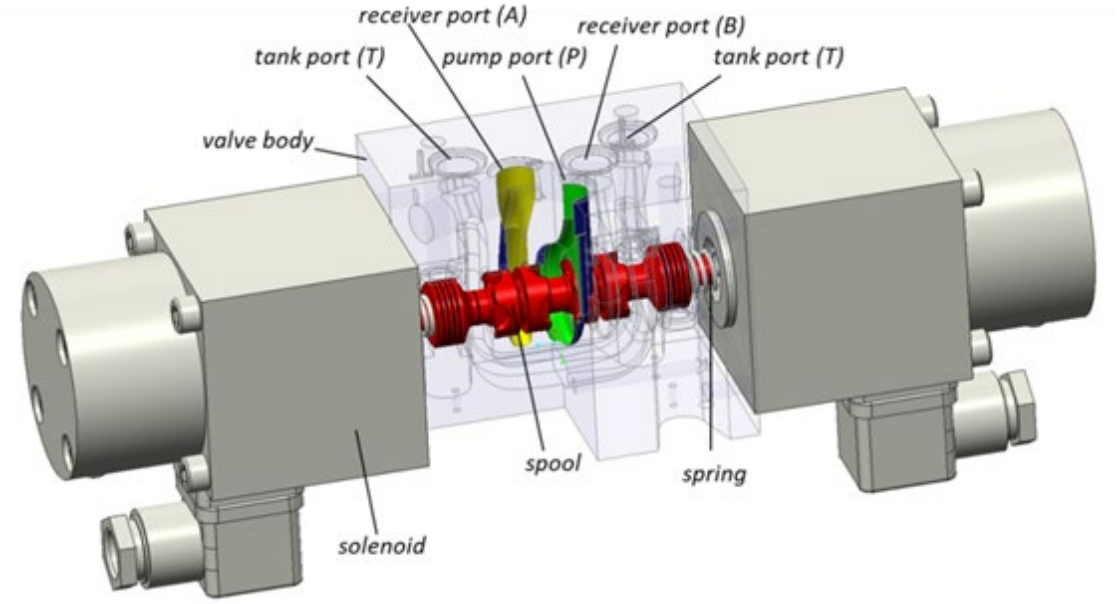

Fig. 1. Spool control valve.

CFD analysis of flow control valve

CFD simulations were conducted in Ansys CFX a general purpose CFD code, which use Finite Volume Method (FVM) for solving flow governing equations and applies multiphase flow model with phase change and Lagrangian particle tracking modelling technique. For numerical simulation path P-A was used with initial opening of 0.3 mm. Boundary conditions and grid is presented in Fig. 3. CFD simulations were performed for cavitation and flow with solid particles independently.

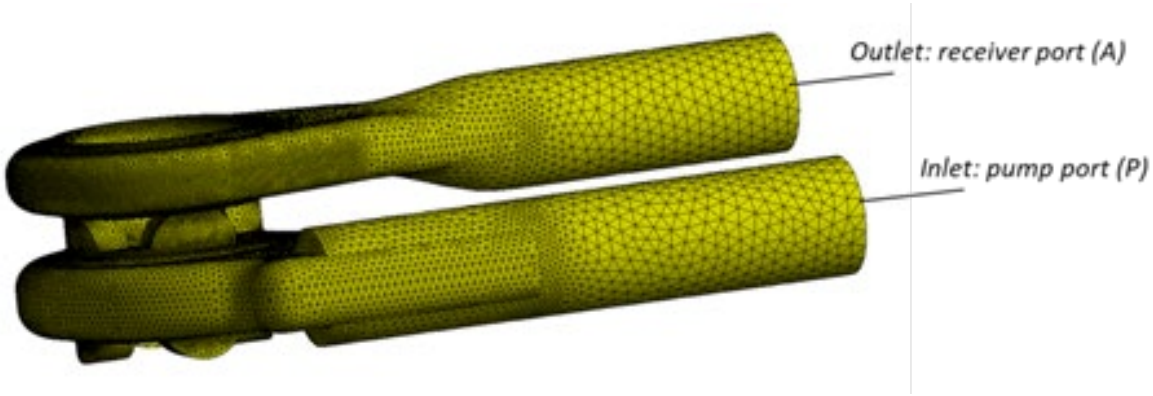

Fig. 2. CFD model: grid and boundary conditions.

CFD simulation was performed for fixed spool position for steady state conditions and for the following assumptions:

– Fluid (hydraulic oil) has a constant properties: density 880 [kg/m^3], viscosity υ=40 [mm^2/s];
– Flow is turbulent: k-ϖ turbulence model was used;
– Model is in thermodynamics equilibrium, heat transfer is not included;

Cavitation simulation included below assumptions:

– Saturation pressure is set to 0.2 [bar];
– Fluid is homogeneous without any dissolved gases;

Whereas particle flow simulation included following assumptions:

– Particles have uniform shape (spheres with diameter 20 [μm]) and constant properties, 20 particles in 1 [cm3];
– Erosion model: Finnie;
– Interaction of particles and fluid is fully coupled;
– Simulations were performed for metallic particles (steel);
– Particles are uniformly injected at inlet to the valve.

Exemplary CFD simulations for solid particle flow are presented in Fig. 3 and Fig. 4. There are presented pathlines of hydraulic oil colored by velocity values and trajectory of solid particles (grey lines).

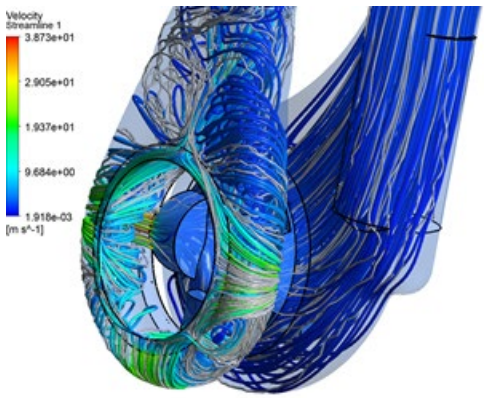

Fig. 3. Fluid path lines (color) and particles trajectory (grey).

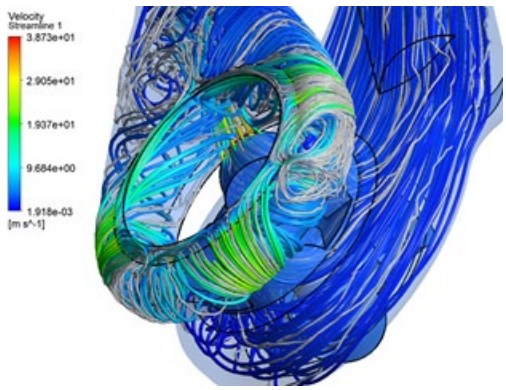

Fig. 4. Fluid path lines (color) and particles trajectory (grey).

Erosion rate density is presented in Fig. 5, which allows to identify areas which are exposed to erosion wear. Figure 6 presents distribution of gas fraction during fluid flow for given conditions.

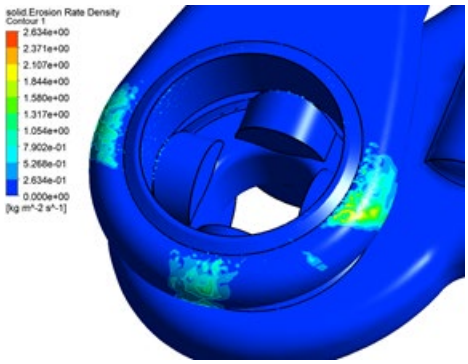

Fig. 5. Erosion rate density.

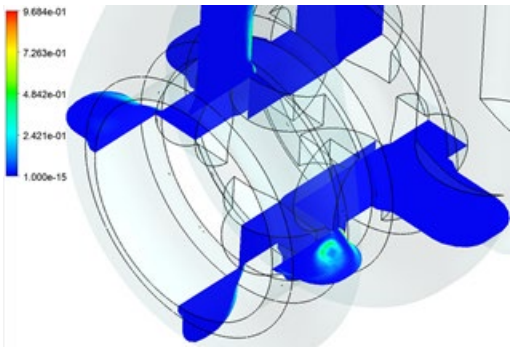

Fig. 6. Oil vapor fraction.

Conclusions

This paper presents attempt of failure prediction of spool control valve caused by contaminated fluid which may cause erosive or cavitation wear. Both are complex phenomena, however, available numerical simulation methods (CFD) allows conducting multiphase flows which includes phase changes (cavitation) and particle tracking. This paper presents simulation of flow inside spool valve for two cases, the first includes hydraulic fluids with metallic contaminants while the second flow with phase changes (cavitation). Obtained results allows to indicate areas which are mostly exposed on wear or to define flow conditions for which wear may occur. CFD simulation tools seem to be an effective tool for perdition of failures in fluid power components.

References

[1] Y. Yaobaoa, Y. Jiayanga, G. Shengrongb, Numerical study of solid particle erosion in hydraulic spool valves, Wear 392-393 (2017) 147-189. https://doi.org/10.1016/j.wear.2017.09.021

[2] X. Liu, H. Ji, W. Min, Z. Zheng, J. Wang, Erosion behavior and influence of solid particles in hydraulic spool valve without notches, Eng. Fail. Anal. 108 (2020) art. 104262. https://doi.org/10.1016/j.engfailanal.2019.104262

[3] Z. Kudzma, M. Stasiak, Studies of flow and cavitation of hydraulic lift valve, Archives of Civil and Mechanical Engineering 15 (2015) 951-961. https://doi.org/10.1016/j.acme.2015.05.003

[4] R. Amirante, E. Distaso, P. Tamburrano, Experimental and numerical analysis of cavitation in hydraulic proportional directional valves, Energy Conversion and Management, 87 (2014) 208–219. https://doi.org/10.1016/j.enconman.2014.07.031

[5] E. Skrzypczak-Pietraszek, K. Reiss, P. Zmudzki, J. Pietraszek, J. Enhanced accumulation of harpagide and 8-O-acetyl-harpagide in Melittis melissophyllum L. agitated shoot cultures analyzed by UPLC-MS/MS. PLOS One. 13 (2018) art. e0202556. https://doi.org/10.1371/journal.pone.0202556

[6] E. Skrzypczak-Pietraszek, K. Piska, J. Pietraszek, Enhanced production of the pharmaceutically important polyphenolic compounds in Vitex agnus castus L. shoot cultures by precursor feeding strategy. Engineering in Life Sciences 18 (2018) 287-297. https://doi.org/10.1002/elsc.201800003

[7] L.J. Orman, Boiling heat transfer on single phosphor bronze and copper mesh microstructures. EPJ Web of Conf. 67 (2014) art. 02087. https://doi.org/10.1051/epjconf/20146702087

[8] A. Tiziani, A. Molinari, J. Kazior, G. Straffelini, Effect of vacuum sintering on the mechanical-properties of copper-alloyed stainless-steel. Powder Metall. 22 (1990) 17-19.

[9] L. Mosinska, K. Fabisiak, K. Paprocki, M. Kowalska, P. Popielarski, M. Szybowicz, A. Stasiak, Diamond as a transducer material for the production of biosensors. Przem. Chem. 92 (2013) 919-923.

[10] D. Klimecka-Tatar, Electrochemical characteristics of titanium for dental implants in case of the electroless surface modification. Arch. Metall. Mater. 61 (2016) 923-26. https://doi.org/10.1515/amm-2016-0156

[11] N. Radek, A. Szczotok, A. Gadek-Moszczak, R. Dwornicka, J. Broncek, J. Pietraszek, The impact of laser processing parameters on the properties of electro-spark deposited coatings. Arch. Metall. Mater. 63 (2018) 809-816.

[12] S. Wojciechowski, D. Przestacki, T. Chwalczuk, The evaluation of surface integrity during machining of Inconel 718 with various laser assistance strategies. MATEC Web of Conf. 136 (2017) art. 01006. https://doi.org/10.1051/matecconf/201713601006

[13] R. Ulewicz, F.R. Novy, The influence of the surface condition on the fatigue properties of structural steel. J. Balk. Tribol. Assoc. 22 (2016) 1147-1155.

[14] D. Malindzak, A. Pacana, H. Pacaiova, An effective model for the quality of logistics and improvement of environmental protection in a cement plant. Przem. Chem. 96 (2017) 1958-1962.

[15] A. Pacana, K. Czerwinska, R. Dwornicka, Analysis of non-compliance for the cast of the industrial robot basis, METAL 2019 28th Int. Conf. on Metallurgy and Materials (2019), Ostrava, Tanger 644-650. https://doi.org/10.37904/metal.2019.869

[16] J. Pietraszek, A. Gadek-Moszczak, The Smooth Bootstrap Approach to the Distribution of a Shape in the Ferritic Stainless Steel AISI 434L Powders. Solid State Phenomena 197 (2012) 162-167. https://doi.org/10.4028/www.scientific.net/SSP.197.162

[17] A. Gadek-Moszczak, J. Pietaszek, B. Jasiewicz, S. Sikorska, L. Wojnar, The Bootstrap Approach to the Comparison of Two Methods Applied to the Evaluation of the Growth Index in the Analysis of the Digital X-ray Image of a Bone Regenerate. New Trends in Comp. Collective Intell. 572 (2015) 127-136. https://doi.org/10.1007/978-3-319-10774-5_12

[18] E. Lisowski, G. Filo, CFD analysis of proportional flow control valve with an innovative opening shape, Energy Conversion and Management 123 (2016) 15-28. https://doi.org/10.1016/j.enconman.2016.06.025

[19] E. Lisowski, G. Filo, J. Rajda, Analysis of flow forces in the initial phase of throttle gap opening in a proportional control valve, Flow Measurement and Instrumentation 59 (2018) 157-167. https://doi.org/10.1016/j.flowmeasinst.2017.12.011

[20] H. Momeni, M. Domagala, CFD simulation of transport solid particles by jet pumps, Technical Transactions 112 (7) 185-191.

[21] M. Domagala, H. Momeni, J. Domagala-Fabis, G. Filo, D. Kwiatkowski, Simulation of Cavitation Erosion in a Hydraulic Valve, Materials Research Proceedings 5 (2018) 1-6. https://doi.org/10.21741/9781945291814-1

[22] M. Domagala, H. Momeni, J. Domagala-Fabis, G. Filo, M. Krawczyk, J. Rajda, Simulation of particle erosion in a hydraulic valve, Materials Research Proceedings 5 (2018) 17-24. https://doi.org/10.21741/9781945291814-4

[23] J. Fabis-Domagała, H. Momeni, G. Filo, M. Domagała, Instruments of identification of hydraulic components potential failures, MATEC Web Conf. 183 (2018) art. 03008. https://doi.org/10.1051/matecconf/201818303008

[24] J. Fabis-Domagala, H. Momeni, M. Domagała, G. Filo, Matrix FMEA analysis as a preventive method for quality design of hydraulic components, CzOTO 1(1) (2019) 684-691. https://doi.org/10.2478/czoto-2019-0087

[25] I.M. Hutchings, Mechanical and metallurgical aspects of the erosion of metals, Conf. Corrosion-Erosion of Coal Conversion System Materials, NACE, Houston, TX (1979) 393-428.

[26] S. Dosanjh, J.A.C. Humphrey, The influence of turbulence on erosion by a particle laden fluid jet, Wear 102 (1985) 309-330. https://doi.org/10.1016/0043-1648(85)90175-9

[27] W. Dosa Tabakoff, G. Grant, R. Ball, An experimental investigation of certain aerodynamics effect on erosion, AIAA Paper No. 74-639, 1974. https://doi.org/10.2514/6.1974-639